



T-Lymphoblastic Lymphoma Cells Express High Levels of BCL2, S1P1, and ICAM1, Leading to a Blockade of Tumor Cell Intravasation

Citation

Feng, Hui, David L. Stachura, Richard M. White, Alejandro Gutierrez, Lu Zhang, Takaomi Sanda, Cicely A. Jette, et al. 2010. T-Lymphoblastic Lymphoma Cells Express High Levels of BCL2, S1P1, and ICAM1, Leading to a Blockade of Tumor Cell Intravasation. *Cancer Cell* 18, no. 4: 353–366.

Published Version

doi:10.1016/j.ccr.2010.09.009

Permanent link

<http://nrs.harvard.edu/urn-3:HUL.InstRepos:13041314>

Terms of Use

This article was downloaded from Harvard University's DASH repository, and is made available under the terms and conditions applicable to Open Access Policy Articles, as set forth at <http://nrs.harvard.edu/urn-3:HUL.InstRepos:dash.current.terms-of-use#OAP>

Share Your Story

The Harvard community has made this article openly available.
Please share how this access benefits you. [Submit a story](#).

[Accessibility](#)



Published in final edited form as:

Cancer Cell. 2010 October 19; 18(4): 353–366. doi:10.1016/j.ccr.2010.09.009.

T-Lymphoblastic Lymphoma Cells Express High Levels of BCL2, S1P1 and ICAM1 Leading to a Blockade of Tumor Cell Intravasation

Hui Feng¹, David L. Stachura², Richard M. White³, Alejandro Gutierrez^{1,3}, Lu Zhang¹, Takaomi Sanda¹, Cicely A. Jette¹, Joseph R. Testa⁴, Donna S. Neuberg⁵, David M. Langenau⁶, Jeffery L. Kutok⁷, Leonard I. Zon³, David Traver^{2,8}, Mark D. Fleming⁹, John P. Kanki¹, and A. Thomas Look^{1,3,*}

¹Department of Pediatric Oncology, Dana-Farber Cancer Institute, Boston, MA 02115, USA

²Cell and Developmental Biology Section, Department of Biological Sciences, University of California at San Diego, La Jolla, CA 92093, USA

³Division of Hematology/Oncology, Children's Hospital, Boston, MA 02115, USA

⁴Cancer Biology Program, Fox Chase Cancer Center, Philadelphia, PA 19111, USA

⁵Biostatistics and Computational Biology, Dana-Farber Cancer Institute, Boston, MA 02115, USA

⁶Department of Molecular Pathology/Cancer Center, Massachusetts General Hospital, Charlestown, MA 02129, USA

⁷Department of Pathology, Brigham and Women's Hospital, Boston, MA 02115, USA

⁸Department of Cellular and Molecular Medicine, University of California at Dan Diego Medical School, La Jolla, CA, 92093, USA

⁹Department of Pathology, Children's Hospital, Boston, MA 02115, USA

Summary

The molecular events underlying the progression of T-lymphoblastic lymphoma (T-LBL) to acute T-lymphoblastic leukemia (T-ALL) remain elusive. In our zebrafish model, concomitant overexpression of *bcl-2* with *Myc* accelerated T-LBL onset while inhibiting progression to T-ALL. The T-LBL cells failed to invade the vasculature and showed evidence of increased homotypic cell-cell adhesion and autophagy. Further analysis using clinical biopsy specimens revealed autophagy and increased levels of BCL2, S1P1 and ICAM1 in human T-LBL compared to T-ALL. Inhibition of S1P1 signaling in T-LBL cells led to decreased homotypic adhesion *in vitro* and increased tumor cell intravasation *in vivo*. Thus, blockade of intravasation and hematologic dissemination in T-LBL is due to elevated S1P1 signaling, increased expression of ICAM1 and augmented homotypic cell-cell adhesion.

*Correspondence: thomas_look@dfci.harvard.edu.

Publisher's Disclaimer: This is a PDF file of an unedited manuscript that has been accepted for publication. As a service to our customers we are providing this early version of the manuscript. The manuscript will undergo copyediting, typesetting, and review of the resulting proof before it is published in its final citable form. Please note that during the production process errors may be discovered which could affect the content, and all legal disclaimers that apply to the journal pertain.

Significance

Thymic lymphomas are closely related to thymic leukemias, but it is unknown why T-LBL remains highly localized as a mediastinal mass in some patients while disseminating rapidly as T-ALL in others. Here we demonstrate that T-LBL cells with increased BCL2 levels possess a distinct cellular phenotype, including impaired vascular invasion, metabolic stress and autophagy. This T-LBL phenotype results from elevated levels of S1P1 and ICAM1 that promote homotypic cell-cell adhesion and block intravasation. Our results show that AKT activation is one mechanism that can overcome the T-LBL block in intravasation, suggesting that PI3K-AKT inhibitors may be helpful in preventing T-LBL cells from acquiring the ability to invade and disseminate.

Introduction

T-lymphoblastic lymphoma (T-LBL) and acute T-lymphoblastic leukemia (T-ALL) are distinct clinical presentations of related malignant diseases that arise in developing thymocytes. The clinical distinction between T-ALL and T-LBL is based on the extent of tumor cell dissemination within the bone marrow and peripheral blood. T-LBL patients typically present with a large anterior mediastinal mass and little evidence of dissemination. However, stage IV T-LBL disease is characterized by distant dissemination through the blood and up to 25% bone marrow cellularity consisting of T lymphoblasts. Cases are classified as T-ALL if the T lymphoblasts comprise more than 25% of the bone marrow cells at presentation, regardless of the extent of thymic or nodal involvement. About one third of T-ALL cases present with a mediastinal mass, while the remaining two thirds lack radiographic evidence of a mediastinal mass and generally have high numbers of circulating T- lymphoblasts (Sen and Borella, 1975; Goldberg et al., 2003). Although T-LBL and T-ALL share many morphologic, immunophenotypic, and genotypic features (Cairo et al., 2005), a recent comparison of T-ALL versus T-LBL gene expression profiles (Raetz et al., 2006) suggests intrinsic differences in growth regulatory pathways that may distinguish between these two malignancies and could be exploited for the development of T-ALL- and T-LBL-specific therapies.

MYC is a potent proto-oncogene that is aberrantly expressed in a broad spectrum of human cancers including leukemia and lymphoma (Nesbit et al., 1999; Pelengaris et al., 2002). In T-ALL and T-LBL, aberrant expression of *MYC* generally occurs downstream of activated NOTCH signaling. Activating mutations in the *NOTCH1* gene have been identified in 40-60% of human T-ALL and 43% of human T-LBL cases, indicating that deregulated *NOTCH1* signaling is major contributor to the pathogenesis of both types of T-lymphoblastic malignancies (Weng et al., 2004; Ferrando et al., 2002; Ferrando, 2009; Park et al., 2009; Pear and Aster, 2004; Shimizu et al., 2007; Weng et al., 2006; Palomero et al., 2006; Sharma et al., 2006). Since *MYC* activates both cell proliferative and apoptotic pathways, tumor cells acquire additional genetic lesions to escape cell death (Meyer et al., 2006; Dang et al., 2005; Asker et al., 1999; Vousden, 2002). Either inactivation of the *p53* pathway or overexpression of *Bcl-2* can cooperate with *Myc* to induce lymphomagenesis in mice (Nilsson and Cleveland, 2003; Hoffman et al., 2002; Pelengaris et al., 2002; Strasser et al., 1990; Eischen et al., 1999).

To identify the critical molecular changes that distinguish T-LBL from T-ALL, we used a zebrafish model to study the fate of transformed thymocyte progenitors. In this system, the vast majority of transgenic fish develop T-LBL progressing rapidly to T-ALL (Langenau 2003Feng et al., 2007), analogous to cases of human T-ALL that present with both a mediastinal mass and high numbers of circulating lymphoblasts. In this report we exploit

this zebrafish model to reveal genetic differences between T-LBL and T-ALL and to uncover the underlying cellular and molecular basis for the divergent clinical pathologies of human T-LBL localized to the mediastinum compared with widely disseminated human T-ALL.

Results

Bcl-2 Accelerates the Onset of Myc-induced T-LBL in Zebrafish

To determine whether *bcl-2* overexpression accelerates the development of Myc-induced T-LBL/ALL in our zebrafish model, we bred double-transgenic (*rag2-LDL-EGFP-mMyc;rag2-EGFP-bcl-2*) heterozygotes with zebrafish transgenic for *Cre* regulated by the heat-shock protein 70 promoter (*hsp70-Cre*), and then monitored disease onset for 129 days after inducing *Cre* expression in the progeny. Despite their similar levels of Myc protein (Figure S1A), the triple-transgenic fish (*Myc;Cre;bcl-2*) developed T-LBL earlier and with a higher penetrance than did their siblings, which expressed only *Myc;Cre*: mean latency, 76 ± 27 (SD) days vs. 103 ± 17 days ($P < 0.0001$; Figure 1A). By 129 days of life, 78% of the triple transgenics but only 37% of the *Myc;Cre* transgenics had developed thymic tumors (Figure 1A). Furthermore, when premalignant GFP-positive T-cells were assayed by Annexin V staining, we found that *bcl-2* expression did indeed inhibit apoptosis in these T-cells (Figure S1B), providing a mechanism through which *bcl-2* collaborates with *Myc* in lymphomagenesis.

Progression of Myc-Induced T-LBL Is Inhibited by Bcl-2 Overexpression

Although *bcl-2* overexpression strikingly accelerated the onset of Myc-induced T-LBL with invasion into local structures (Figures 1A and 1F), progression of the thymic lymphomas to disseminated leukemias was inhibited in these transgenics (Figures 1B and 1F-H), compared with the *Myc*-only line (Figures 1B-E). By 261 days of life, only 24% of the *Myc;Cre;bcl-2* fish with T-LBL had shown progression to T-ALL, in marked contrast to the nearly 100% rapid dissemination rate in fish that expressed only *EGFP-mMyc* ($P = 0.0002$; Figures 1B, 1D-E, and 1G-H). To further explore the differences in dissemination rates, we transplanted equal numbers of GFP-sorted control thymocytes or lymphoma/leukemic cells intraperitoneally into irradiated wild-type recipients. While nontransformed control *rag2-EGFP-bcl-2* thymocytes did not survive transplantation (data not shown), both *Myc;Cre* and *Myc;Cre;bcl-2* tumor cells were readily transplantable, as shown by EGFP-labeled tumor cells in the abdomens of fish at 2 weeks post-transplantation (Figures 1I and 1K). T-LBL cells from most *Myc;Cre;bcl-2* transgenics remained localized in the abdomens of transplanted recipients and did not metastasize to other regions (Figure 1L), while the transplanted *Myc;Cre* tumor cells showed widespread dissemination by 6 weeks post-transplantation (Figure 1J).

Bcl-2-overexpressing Lymphomas Are Defective in Vasculature Intravasation

To further examine the different fates of *Myc;Cre* versus *Myc;Cre;bcl-2* tumor cells *in vivo*, we studied tissues from sacrificed fish. The *rag2-GFP* fish were sectioned as controls and stained with hematoxylin and eosin (H&E). The control group showed thymocytes residing in the thymus, without local invasion into the gills or other perithymic structures (Figures 2A, 2E, and 2I). By contrast, both young (Figures 2B and 2F) and old (Figures 2C and 2G) *Myc;Cre;bcl-2* fish showed extensive local infiltration into the gill structures, operculum and other regions surrounding the thymus, a finding confirmed by immunostaining for GFP (data not shown). Interestingly, the malignant *Myc;Cre;bcl-2* lymphoblasts extended from the thymus along subepithelial interstitial spaces, but they failed to invade the vasculature and were not evident in the nearby red blood cell-containing capillaries of the gills (Figures 2J-K). In *Myc;Cre* fish several months of age, lymphoblasts extensively invaded the

perithymic region surrounding the gills (Figures 2D, 2H, and 2L), including the central capillary network within the secondary gill lamellae (Figure 2L). As we have reported (Langenau et al., 2003), these cells were also widely disseminated and invaded the tissues in organ systems throughout the fish, including nonhematopoietic tissues such as distant muscle, liver, intestine, and testis. Taken together, these results indicate that the *Myc;Cre;bcl-2* tumor cells arising in the majority of the transgenic fish are impaired in their ability to disseminate into the vascular system from the thymus, although they are locally invasive and disseminate by extension through contiguous interstitial spaces around the thymus.

To further elucidate how *bcl-2*-overexpressing lymphoma cells disseminate by invasion across tissue planes without intravasating into the microvasculature, we monitored the *in vivo* behavior of lymphoma cells isolated from *Myc;Cre* and *Myc;Cre;bcl-2* transgenic zebrafish, by combining transplantation assays with *in vivo* confocal imaging. Due to the incomplete excision of the *loxP-dsRED2-loxP* cassette from the *Myc (rag2-LoxP-dsRED2-LoxP-EGFP-mMyc)* transgene (Feng et al., 2007), cells from *Myc;Cre* and *Myc;Cre;bcl-2* tumors both express *dsRED2* together with *EGFP*. The presence of *dsRED2* allowed the visualization of these tumor cells within the context of adult host *fli1-EGFP;Casper* fish, which are transparent and express *EGFP* much stronger in the vasculature than do the tumor cells, allowing lymphoma cell intravasation to be monitored *in vivo*. When equal numbers of FACS-sorted *Myc;Cre* or *Myc;Cre;bcl-2* T-LBL cells were transplanted into *fli1-EGFP;Casper* fish, tumor cells were readily apparent at 6 days post-transplantation and were assayed by confocal microscopy for dissemination and vascular intravasation. At that time, many more *Myc;Cre* tumor cells relative to *Myc;Cre;bcl-2* T-LBL cells had invaded blood vessels (Figures 2M-R), despite the fact that most of the latter cells were in close proximity to the vessels (Figures 2P-R). To quantify this effect, we calculated the percentages of intravasating *Myc;Cre;bcl-2* and *Myc;Cre* lymphoma cells: mean 0.56 ± 0.80 (SD) versus 1.66 ± 0.99 , respectively (n=17 and 20; $P < 0.0001$). Unlike the majority of transplanted *Myc;Cre;bcl-2* tumor cells, those expressing *Myc;Cre* circulated in blood vessels throughout the animal at 12 days post-transplantation and were associated with a large tumor burden. Although difficult to quantify, the transplanted *Myc;Cre;bcl-2* T-LBL cells also showed increased formation of cellular aggregates (see Figures 2Q-R).

Zebrafish T-LBL Cells Overexpressing *Bcl-2* Undergo Autophagy

To further examine the difference in lymphoma cells with or without *bcl-2*-overexpression, we compared the morphology and cell cycle status of GFP-sorted thymocytes from i) *GFP* control (*rag2-GFP*), ii) *bcl-2* control (*rag2-EGFP-bcl-2*), iii) *Myc;Cre;bcl-2* and iv) *Myc;Cre* transgenic fish (Figures S2A-D). The malignant thymocytes expressing the *rag2-EGFP-bcl-2* transgene were smaller than cells transformed by the *Myc* transgene alone (Figures S2C-D and S7N). Moreover, cell cycle analysis revealed that T-LBL cells from the *Myc;Cre;bcl-2* transgenic fish had a much lower proliferative fraction (0.65% in S-phase) compared with control *GFP* (9.31%), *bcl-2* (10.27%) thymocytes or with tumor cells from the *Myc;Cre* transgenic fish (10.8%) (Figure S2E). These characteristics could reflect metabolic stress and autophagy, so *Myc;Cre* and *Myc;Cre;bcl-2* lymphoma cells were assessed by transmission electron microscopy. Interestingly, T-LBL cells overexpressing *bcl-2* had significantly more autophagosomes/autolysosomes than *Myc;Cre* tumor cells: 2.7 ± 2.0 (SD) versus 0.23 ± 0.58 per cell section ($P < 0.0001$; Figure 3A-E).

Microtubule-associated protein 1 light chain 3 (LC3), served as a marker for autophagy (Kabeya et al., 2000) and its active form, Lc3-II, was abundant in *Myc;Cre;bcl-2* lymphoma cells but not in *Myc;Cre* lymphoma cells (Figure 3F). *Myc;Cre* tumors also failed to express the precursor form, Lc3-I, consistent with the *LC3* gene being transcriptionally upregulated only when cells undergo autophagy (Donati et al., 2008; Yasmeen et al., 2003). These

findings show that autophagy is triggered as a catabolic survival mechanism specific to *Myc;Cre;bcl-2* tumor cells.

To test whether autophagy contributed to the inability of zebrafish *bcl-2*-overexpressing lymphoma cells to disseminate, we treated control wild-type fish, and *Myc;Cre* and *Myc;Cre;bcl-2* transgenic fish with the autophagy inhibitor chloroquine (CQ), which was well-tolerated by both wild-type and tumor-bearing fish at a concentration up to 100 μ M. As expected (Amaravadi et al., 2007), autophagosomes/autolysosomes could not metabolize their contents, resulting in their significantly increased numbers in CQ-treated T-LBL cells compared to controls (mean: 17.9 ± 10.7 (SD) vs. 5.8 ± 3.8 , $P < 0.0001$; Figures S3A-E). However, none of the T-LBL cells in *Myc;Cre;bcl-2* fish disseminated over 12 weeks of treatment with CQ (Figures S3F-I), indicating that autophagy is not responsible for the lack of T-LBL cell dissemination.

AKT Activation Promotes the Progression of T-LBL to T-ALL in Zebrafish

AKT activation by phosphorylation is known to promote T-cell migration and nutrient uptake, to relieve metabolic stress, and to suppress autophagy (Sotsios and Ward, 2000; Lum et al., 2005), suggesting its involvement in the progression of T-LBL to T-ALL. We therefore examined the levels of phospho-Akt (Ser473p-Akt) in lymphoma cells in two separate experiments with i) *Myc;Cre;bcl-2* transgenic fish in which tumors remained localized as T-LBL (n=5); ii) leukemic cells from the 24% of *Myc;Cre;bcl-2* fish in which the cells disseminated as T-ALL (n=6); and iii) leukemic cells expressing *Myc;Cre* alone (n=6; Figure 4A and data not shown). In both experiments, there were striking increases in Ser473p-Akt, indicating elevated levels of phosphorylated Akt in *Myc;Cre;bcl-2* tumors that had disseminated as T-ALL. This was in marked contrast to the low levels of Ser473p-Akt observed in T-LBL tumor cells that remained confined locally around the thymus. Levels of Ser473p-Akt and Lc3-II (Figure 4A, lanes 6-8) were consistently low in the *Myc;Cre* leukemic cells, suggesting that Akt activation was not required by these tumor cells to promote intravasation and dissemination.

To test experimentally whether Akt activation can promote the progression of T-LBL to T-ALL, we introduced a constitutively active, myristoylated murine *Akt2* (*Myr-Akt2*) transgene driven by the *rag2* promoter into the *Myc;Cre;bcl-2* transgenic fish by microinjection at the 1-cell stage. Tumor cells from all four fish tested with constitutive expression of *Myr-Akt2* had increased Ser473p-Akt levels, as did one of the four fish without *Myr-Akt2* expression (Figure 4B). Constitutively activated Akt promoted more rapid onset of T-LBL in the *Myc* transgenic fish with or without *bcl-2* overexpression (Figure S4), and more rapid dissemination of T-LBL to T-ALL in the *Myc;Cre;bcl-2;Myr-Akt2* transgenic fish (Figures 4E-G). By 217 days of life, 85% of the *Myc;Cre;bcl-2;Myr-Akt2* transgenic fish with T-LBL had developed T-ALL, in marked contrast to only 30% of the *Myc;Cre;bcl-2* transgenic fish with T-LBL (Figure 4G). Dissemination was more rapid, as the earliest time that the *Myc;Cre;bcl-2;Myr-Akt2* transgenic fish developed T-ALL was 34 days of life, compared to 114 days for their *Myc;Cre;bcl-2* siblings.

Human T-LBL Cells Undergo Autophagy

To test whether human T-LBL, but not T-ALL, lymphoblasts undergo autophagy, as predicted by our zebrafish model, we performed western blot analysis to examine expression of the autophagy protein LC3-I and its active LC3-II isoform (Kabeya et al., 2000; Donati et al., 2008; Yasmeen et al., 2003). Relative to the T-ALL cases, the T-LBL cases showed high levels of LC3-I and LC3-II (Figure 5A), indicating that human T-LBL lymphoblasts were actively undergoing autophagy. We confirmed this finding by demonstrating higher levels of another protein indicative of autophagy, BECLIN 1 (ATG6) (Cao and Klionsky, 2007),

which is transcriptionally upregulated when cells undergo autophagy (Donati et al., 2008; Cao and Klionsky, 2007; Yan et al., 2007), in T-LBL compared to T-ALL samples (Figure 5A). In autophagic cells, the LC3-II isoform is sequestered in autophagosomes, allowing its subcellular localization to be detected by immunofluorescence assays (Kabeya et al., 2000). LC3 was expressed at low diffuse levels in the cytoplasm of normal T-cells (Figures 5G and 5J) and of the lymphoblasts in 10 of 11 T-ALL bone marrow samples (Figures 5I and 5L; Figure S5C). However, strong punctate LC3 staining was observed in 7 of 9 T-LBL cases examined (Figures 5H and 5K; Figure S5C), further supporting subcellular sequestration of LC3 and the specific induction of autophagy in human T-LBL but not T-ALL lymphoblasts.

Human T-LBL Cells Overexpress *BCL2α*, *S1P1*, and *ICAM1*

Our zebrafish data suggest that a difference in *BCL2* expression may represent an important distinction between human T-LBL and T-ALL. The human *BCL2* protein has two isoforms that are produced by alternatively spliced transcripts. The widely studied antiapoptotic *BCL2α* isoform contains 239 amino acids and a hydrophobic carboxy-terminal transmembrane domain (TM) (Figure S5A). This membrane anchor is lacking in the 205-amino-acid *BCL2β* isoform (Figure S5A), which appears to lack antiapoptotic activity (Tanaka et al., 1993). The zebrafish *bcl-2* transgene used in this study is most similar to the human *BCL2α* isoform.

To determine whether *BCL2α* is differentially expressed in primary human T-LBL and T-ALL cells, we analyzed recently published RNA expression profiling results obtained from 9 T-LBL and 10 T-ALL samples (Raetz et al., 2006). Expression of *BCL2α* in human T-LBL was significantly higher than that in T-ALL (Figure 5C and Table S1). To determine if T-LBL samples had higher *BCL2α* protein levels, we extracted proteins from six T-LBL and seven T-ALL primary patient samples and subjected them to Western blot analysis. The Du528 T-ALL cell line, which expresses both *BCL2α* and *BCL2β* was used as a control to show the relative migration of the two isoforms (Figure S5B). Analysis of this Western blot (Figure S5B) showed that *BCL2α* levels were significantly higher ($P=0.038$) in T-LBL versus T-ALL samples ($BCL2α/ACTIN$ ratio mean: 0.29 ± 0.07 (SD) vs. 0.09 ± 0.02 ; Figure 5D), while there were no detectable differences in the expression levels of other antiapoptotic proteins, such as *MCL1* and *BCLXL* (Figure 5A and Table S1).

To extend our analysis of *BCL2* expression in lymphoblastic lymphoma cells, we performed immunohistochemical analyses of normal and T-LBL human thymic tissue biopsies, together with T-ALL specimens from bone marrow biopsies (Figure 6). While both T-LBL and T-ALL samples contained mature T-cells with strong *BCL2* expression, the normal thymic architecture in the T-LBL samples was clearly disrupted, and 7 of 11 of these samples showed high levels of *BCL2* expression in the tumor cells (Figures 6B, 6E and S6). By contrast, *BCL2* levels were essentially undetectable in the lymphoblasts from 10 of 11 T-ALL samples (Figures 6C and 6F). Our analysis demonstrates that *BCL2* levels are significantly higher in human T-LBL compared to those of T-ALL cells, a finding that is consistent with the predictions of our zebrafish model. To address whether the difference in *BCL2* levels between T-LBL and T-ALL might reflect altered stages of T-cell development, we performed immunohistochemical assays of the CD3, CD4, and CD8 surface antigens, but did not identify any differences in the patterns of expression between these two disease types (see Table S2).

Although increased expression of *BCL2* in T-LBL cells may contribute to the onset of lymphoma, it does not explain why in many of these cases the transformed cells fail to invade the vasculature and disseminate. To address this question, we analyzed the published gene expression data of Raetz and coworkers using Gene Set Enrichment Analysis (GSEA) to see if the curated gene sets for integrin mediated cell adhesion, cell adhesion molecules

and leukocyte transendothelial migration were differentially expressed in T-LBL versus T-ALL (Raetz et al., 2007; Mootha et al., 2003). Although GSEA analysis failed to reveal significant enrichment for any of these three gene sets (<http://www.broadinstitute.org/gsea/msigdb/index.jsp>) between T-LBL (n=9) and T-ALL (n=10) patient samples, some individual genes within these gene sets did exhibit differential expression. After including additional candidate genes reported in the literature, we focused our efforts on 6 proteins involved with T-lymphocyte adhesion and migration, which included S1P1, ICAM1 (the downstream target of S1P1), and its receptor LFA1, E2 (CD99), N-cadherin, and E-cadherin (Petrie and Zuniga-Pflucker, 2007; Rosen and Goetzl, 2005a; Makgoba et al., 1988; Bernard et al., 1995; Kawamura-Kodama et al., 1999). While our Western blot analysis failed to detect significant differences in the expression levels of 4 of the 6 molecules tested, significant increases in S1P1 and ICAM1 levels were observed in T-LBL relative to T-ALL cells: S1P1/ACTIN ratio, mean 2.96 ± 1.90 (SD) vs. 0.77 ± 1.19 , $P=0.04$ (Figures 5A and 5E); ICAM1/ACTIN ratio, mean 1.67 ± 0.96 (SD) vs. 0.07 ± 0.09 , $P=0.007$ (Figures 5B and 5F). These results are interesting because S1P1 signaling promotes homotypic T cell adhesion and inhibits thymocyte emigration and endothelial intravasation, at least in part through S1P1's ability to upregulate ICAM1 levels (Makgoba et al., 1988; Rosen et al., 2009b; Lin et al., 2007).

To extend our Western blot results to additional cases, we examined S1P1 expression levels by immunohistochemical analysis of normal thymus, T-LBL tumor biopsies and T-ALL bone marrow biopsies. As shown in Figures 6A and 6D, BCL2 is normally not detectable in immature thymocytes in the thymic cortex, and then is markedly upregulated to promote the survival of more mature single-positive thymocytes in the medulla that are ready to egress via the circulation. By contrast, S1P1 is expressed by cortical thymocytes and is downregulated as more mature thymocytes traffic to the medulla (Figures 6G and 6J). In the T-LBL cases, S1P1 is expressed at levels comparable to the high levels normally expressed by immature cortical thymocytes that are retained in the thymus (Figures 6H and 6K, Figure S6, and Table S2), while BCL2 levels are aberrantly upregulated similar to more mature thymocytes in the thymic medulla (Figures 6B and 6E, and Table S2). By contrast, only a small subset T-ALL cells expressed detectable levels of S1P1 (Figures 6I and L, Figure S6, $P=0.03$). These results show that the high S1P1 levels observed on human T-LBL cells most closely resemble the levels that found on immature normal cortical thymocytes that are retained in the thymus, while human T-ALL lymphoblasts with low S1P1 levels resemble those that are able to emigrate from the thymus into the circulation.

***Bcl-2*-Overexpressing T-LBL Cells Exhibit Increased Aggregation That Can Be Overcome by Akt Activation or S1P1 Inhibition**

To gain further insight into the failure of T-LBL cells to disseminate in *Myc;Cre;bcl-2* transgenic fish, we analyzed the phenotypic behavior of these sorted tumor cells *in vitro*. Tumor cells from both *Myc;Cre* and *Myc;Cre;bcl-2* transgenic fish were unable to survive *in vitro* without the support of a zebrafish kidney stromal cell line (ZKS) (Stachura et al., 2009; data not shown). Growing on a monolayer of ZKS cells, T-LBL cells overexpressing *bcl-2* and *Myc* survived far better than did their counterparts overexpressing *Myc* alone, under both normal and hypoxic conditions. Compared to T-LBL cells overexpressing *Myc* alone, which die by 12 days in culture, T-LBL cells overexpressing *bcl-2* and *Myc* can routinely survive for over 2 months. The *Myc;Cre;bcl-2* lymphoma cells were significantly smaller than *Myc;Cre* cells under both normal (mean \pm SD cell diameter, 1.79 ± 0.59 μm vs. 3.33 ± 1.50 μm) and hypoxic (1.62 ± 0.55 μm vs. 3.30 ± 1.46 μm) conditions ($P<0.0001$, Figure S7N), consistent with their autophagic state, which may promote their survival under both *in vivo* and *in vitro* conditions. *Myc;Cre* cells appeared large and apoptotic, expressed the apoptotic marker Annexin V on their surface (Figure S7P), and were noticeably less healthy

after 8 days in culture, particularly under hypoxic conditions (Figure S7L). These observations demonstrate that *Myc;Cre;bcl-2* T-LBL cells have a survival advantage over *Myc;Cre* cells.

Interestingly, when cultured *in vitro*, single FACS-sorted lymphoma cells from the majority of *Myc;Cre;bcl-2* transgenic fish formed aggregates (over 10 cells per aggregate) in standard (Figures 7C and 7F) as well as hypoxic (Figure S7F) culture conditions. In contrast, malignant cells from all *Myc;Cre* transgenic fish failed to form aggregates under the same conditions (Figures 7B and 7F). The number of *Myc;Cre;bcl-2* T-LBL cell aggregates increased over time and was not dependent upon initial plating densities (Figures S7A-E and S7M), compared to *Myc;Cre* lymphoma cells (Figure S7G-K). Furthermore, the numbers of viable lymphoma cells did not significantly increase over a week in culture (Figure S7O), indicating that the formation and increased numbers of aggregated *Myc;Cre;bcl-2* T-LBL cells was not due to increased proliferation. These cells survived over 2 months *in vitro* and still retained the ability to aggregate (data not shown).

To examine whether the T-LBL aggregation phenotype could be overcome by Akt activation, we cultured tumor cells from both the 24% of *Myc;Cre;bcl-2* transgenic fish with endogenous Akt activation that progressed to T-ALL and the *Myc;Cre;bcl-2;Myr-Akt2* transgenic fish. Importantly, leukemic cells from most of the *Myc;Cre;bcl-2* or *Myc;Cre;bcl-2;Myr-Akt2* fish failed to aggregate (Figures 7D-F), as compared to the T-LBL cells from the 76% of *Myc;Cre;bcl-2* transgenic fish that remained localized, indicating that Akt activation is able to overcome the aggregating properties of *Myc;Cre;bcl-2* lymphoma cells and that the abrogation of *in vitro* aggregation appears to be linked to the cells' capacity to disseminate.

Because S1P1 was overexpressed by human T-LBL cells, and the ligand-binding domain of zebrafish *s1p1* is also highly conserved, we tested whether the S1P1 pathway regulated the cellular aggregation phenotype of zebrafish *Myc;Cre;bcl-2* T-LBL cells, using W146, a specific S1P1 antagonist (Sanna et al., 2006), to treat malignant cells from transgenic fish. While W146 treatment had no detectable effect on the malignant cells from *Myc;Cre* fish (data not shown), it caused a marked reduction in the aggregation of *Myc;Cre;bcl-2* T-LBL cells without affecting cell survival (Figures 7G-K; data not shown). These results indicate that the homotypic cell-cell aggregation of the *bcl-2*-overexpressing T-LBL cells depends upon S1P1 signaling.

S1P1 Antagonist Treatment Promotes the Intravasation of *Bcl-2*-overexpressing T-LBL Cells *in Vivo*

To establish whether the S1P1 signaling pathway regulates the ability of *Myc;Cre;bcl-2* lymphoma cells to intravasate into the microvasculature, we treated *Myc;Cre;bcl-2* transplants *in vivo* with the W146 S1P1 inhibitor (Figure 8A). Twelve days after transplantation, either a control vehicle solution or the W146 inhibitor was injected into the host *Fli1-EGFP;Casper* fish at the cell transplantation site. Three days later, the fish were examined by confocal microscopy and scored for dissemination and intravasation. Minimal intravasation of the transplanted cells was observed in the vehicle-treated fish (Figures 8B-D), while the W146-treated fish showed significantly higher numbers of intravasating tumor cells (Figures 8E-G; mean \pm SD intravasation score, 0.89 ± 0.83 versus 2.07 ± 0.86 , respectively, $P < 0.0001$). Similar to what was observed previously (Figures 2Q and 8C), the transplanted *Myc;Cre;bcl-2* T-LBL cells formed aggregates *in vivo* in the control-treated fish, while the W146 treatment led to a dissociation of the cell aggregates (Figure 8F). These results indicate that inhibition of S1P1 signaling can restore the capacity for *Myc;Cre;bcl-2* lymphoma cells to disaggregate and intravasate into the vasculature *in vivo*, thus implicating

high S1P1 levels in the blockade of dissemination observed in zebrafish T-LBL and by extension in human patients with this disease.

Discussion

Our studies in zebrafish define the cellular and molecular differences between human T-LBL and T-ALL, providing for a biological basis for the different clinical presentations of these two T-cell malignancies. The results indicate that aberrant overexpression of *BCL2* together with *MYC* accelerates the onset of malignant transformation by suppressing Myc-induced apoptosis (Strasser et al., 1990), while elevated S1P1 and ICAM1 levels promote homotypic cell adhesion through binding to LFA1, associated with a blockade of intravasation and thymic egress. The transformed T-LBL lymphoblasts that are unable to intravasate and undergo hematologic dissemination remain trapped in the thymic region, where they proliferate to the capacity of their local nutrient supply and induce the autophagy program in response to metabolic stress. Conversely, *MYC*-stimulated lymphoblasts with low levels of *BCL2* expression appear to undergo a more protracted multistep transformation process that may involve activation of alternative cell survival programs, as well as molecular pathways that promote dissemination outside of the thymic environment. These T-ALL lymphoblasts rapidly undergo hematologic dissemination to nutrient rich environments throughout the host, thus avoiding metabolic stress and the induction of autophagy.

Thymocytes express a number of adhesion molecules, including N-cadherin, E-cadherin, ICAM1, and LFA1, during specific stages of maturation that are associated with specific functions including thymocyte emigration and intravasation (Petrie and Zuniga-Pflucker, 2007; Boyd et al., 1988). The regulated expression of ICAM1 controls the balance of homotypic cell-cell adhesion and heterotypic adhesion to vascular endothelial cells, which modulates the intravasation process (Boyd et al., 1988; Guo et al., 2009; Gares and Pilarski, 2000). Recent evidence supports the contribution of S1P1 function to the process of thymocyte intravasation through its regulation of ICAM1 levels (Lin et al., 2007), and S1P1 agonists such as SEW2874 have been shown to increase S1P1 signaling in the thymus and inhibit mature thymocyte egress (Sanna et al., 2006). Consistent with these data, we show that T-LBL cases overexpressing BCL-2 have high S1P1 levels mirroring those of immature cortical thymocytes that do not emigrate from the thymus (Figure 6G). The mechanism underlying this association is uncertain, but it does not appear to be solely dependent on the state of thymocyte differentiation, since cases of both T-ALL and T-LBL can present with cell surface markers indicating arrested T-cell development at all maturation stages (Crist et al., 1988). Our experiments also show that the W146 S1P1 inhibitor reduces homotypic thymocyte cell-cell adhesion and implicate the loss of homotypic cell-cell adhesion in the ability of T-LBL cells to intravasate in our *in vivo* transplantation assays. The evidence of elevated S1P1 and ICAM1 expression in human T-LBL cells, together with evidence for S1P1-dependent cell aggregation *in vitro* and *in vivo*, strongly support a role of homotypic cell adhesion mediated through elevated ICAM1, in regulating T-LBL intravasation and subsequent hematologic dissemination.

Our results suggest that the induction of autophagy is a consequence rather than a cause of the inability of malignant T-lymphoblasts to disseminate in our zebrafish model. First, when zebrafish *Myc; Cre; bcl-2* T-LBL cells were cultured *in vitro*, their survival indicated that their inability to disseminate could not be attributed to their inability to survive outside the thymic niche. Second, inhibitors of autophagy failed to restore the ability of T-LBL cells to disseminate.

While low levels of activated Akt were observed in *Myc;Cre;bcl-2* zebrafish with localized T-LBL lymphomas, the *Myc;Cre;bcl-2* lymphomas that progressed to T-ALL possessed high levels of phospho-Akt (Ser 473-p-Akt), suggesting that AKT activation provides a mechanism allowing *bcl-2*-overexpressing cells to disseminate. Furthermore, the expression of a constitutively active form of murine *Akt2* (*Myr-Akt2*) in *Myc;Cre;bcl-2* transgenic zebrafish promoted rapid dissemination of the disease while lymphoblasts overexpressing Akt failed to aggregate *in vitro*, further supporting the association between activated Akt signaling, the loss of cell adhesion and T-ALL dissemination.

Human T-ALL and T-LBL are considered to represent different clinical presentations of the same disease that are often treated with identical treatment regimens. Our studies suggest that different molecular and cell biologic properties may render these diseases uniquely susceptible to different types of targeted therapies. Thus in T-LBL patients, combination of BCL2 and AKT inhibitors could promote lymphoblast death while blocking pathways that lead to lymphoblast escape and dissemination. Such approaches would likely have little efficacy for the majority of patients with T-ALL, who have low levels of BCL2 expression and lack evidence of activation of autophagy. Our studies also suggest that BCL2 levels, AKT phosphorylation, and LC3 and BECLIN1 levels should be carefully analyzed in future clinical trials, to determine whether these biomarkers predict clinical response and implicate pathways for targeted therapy.

Experimental Procedures

Fish Husbandry

Zebrafish husbandry was performed as described (Westerfield, 1994) in the Dana-Farber zebrafish facility, in accord with our ACUC-approved protocol.

Overexpression of *Myc*, *bcl-2*, and *Myr-Akt2* in Zebrafish Lymphocytes, Tumor Screen, and Fish Genotyping

To test the cooperative effect of *bcl-2* and *mMyc*, we bred double-transgenic fish, *rag2-EGFP-bcl-2;rag2-LDL-EGFP-mMyc*, to homozygous *hsp70-Cre* fish; To overexpress *Myr-Akt2* in lymphocytes, we injected the ISceI-*Rag2-Myr-Akt2*-ISceI construct with the I-SceI meganuclease into one-cell-stage embryos from the same breeding scheme described above. All resulting progeny were heat-shocked and raised, monitored for T-LBL onset and genotyped as described (Feng et al., 2007). Thymocytes were dissected for DNA extraction and genotyped from fish injected with the ISceI-*rag2-Myr-Akt2*-ISceI construct. Genotyping primer information is included in Supplemental Experimental Procedures.

Analysis of Zebrafish Lymphoma and Leukemic T cells

Control (from *rag2-GFP* and *rag2-EGFP-bcl-2*) or transformed T cells (from *Myc;Cre*, *Myc;Cre;bcl-2* or *Myc;Cre;bcl-2;Myr-Akt2*) were collected under a UV-dissection scope (Leica) and sorted on the basis of dsRED2/GFP expression. The sorted cells were subjected to: 1) transplantation into recipients (0.7 million cells per fish) as described (Langenau et al., 2005); 2) electron microscopic analysis to determine the presence and number of autophagosomes and autolysophagosomes per cell section (Nine to 15 different cell sections were obtained for each *Myc;Cre* and *Myc;Cre;bcl-2* fish); or 3) *in vitro* culture to assay aggregation properties (See Supplemental Experimental Procedures for details).

Small Molecule Treatment and Confocal Imaging

The S1P1 antagonist W146 or the control vehicle was added to the cultured dsRED2/GFP-sorted lymphoma cells and cell aggregation was assayed as described in the Supplemental Experimental Procedure section. For *in vivo* treatment, W146 or vehicle was injected into

the host *Fli1-EGFP;Casper* fish that had received *Myc;Cre;bcl-2* lymphoma cells. Transplant recipients were examined for EGFP (blood vessels) and dsRED2 (tumor cells) by confocal imaging. Each image was scored on a 0 to 3 scale that estimated the fraction of tumor cells contained within a blood vessel, as follows: 0=no cells in blood vessels, 1= \leq 25% of cells in blood vessels, 2=25-75% in blood vessels, and 3=100% in blood vessels.

Patient Samples

Diagnostic bone marrow specimens were collected with informed consent and with approval of the Dana-Farber Cancer Institute Institutional Review Board from children with T-ALL enrolled in Dana-Farber Cancer Institute clinical trials for pediatric ALL. T-LBL diagnostic specimens were removed at surgery from patients diagnosed at Children's Hospital Boston who gave informed consent for use of anonymized surgical specimens for research purposes after all clinically relevant evaluations were performed, with approval of the Children's Hospital Boston Institutional Review Board. All samples are reported by arbitrary Sample ID numbers without linked identifiers (Table S2) and were analyzed with approval of the Dana-Farber Cancer Institute Institutional Review Board. Mononuclear tumor cells were isolated from T-ALL bone marrow specimens by Ficoll-Hypaque density centrifugation. The diagnosis of T-ALL or T-LBL was made by each institution's pathologists and clinicians based on criteria of the World Health Organization.

Western Blot Analysis

The primary antibodies included anti-BCL2, anti-CD3, anti-CD4, and anti-CD8 (Santa Cruz), anti-BCLXL (BD Biosciences), anti-MCL1 (BD Biosciences), anti-LC3 (MBL International Co.), anti-LC3 β (Abcam), anti-BECLIN1 (ANASPEC Inc.), anti-S1P1 (Novus Biologicals), anti-AKT, anti-phosph Ser473-AKT, anti-ICAM1, anti-N-Cadherin, anti-E-Cadherin (Cell Signaling), anti-LFA1 (LifeSpan Biosciences), and anti-ACTIN (Sigma) antibodies. Secondary antibodies included horseradish peroxidase-conjugated anti-mouse or anti-rabbit antibodies (Pierce). Autoradiographs were either exposed directly to CL-exposure film (Pierce) and then scanned with a MICROTEK Deskscan or were imaged with a G:BOX chemi HR16 device (Syngene) and a CCD camera, and then subjected to analysis with Syngene genetool software.

Immunohistochemistry and Immunofluorescence Staining

See Supplemental Experimental Procedures for detailed descriptions.

Statistical Analysis

Kaplan-Meier analysis and the log-rank test were used to compare times to T-LBL or T-ALL onset among groups of fish. The exact Wilcoxon rank-sum statistic was used to compare aggregates over free cells among lymphoma and leukemic cells from different transgenic fish. Fisher's exact test was used to analyze differences in BCL2 α , LC3, and CD3/CD4/CD8 staining in clinical samples of T-LBL versus T-ALL lymphoblasts. Student's t test was used to analyze differences in EGFP-mMyc levels, annexin V positive cells, S-phase cells, cell size, autophagosome number in *Myc;Cre* versus *Myc;Cre;bcl-2* tumor cells, control- or chloroquine-treated *Myc;Cre;bcl-2* tumor cells, the BCL2/ACTIN, S1P1/ACTIN, and ICAM1/ACTIN protein ratio, and the percentage of S1P1-positive-cells of patient T-LBL samples versus T-ALL samples. Student's t test was also used to analyze differences in W146-treatments for zebrafish tumor cells in cell culture and the intravasation scores between *Myc;Cre* and *Myc;Cre;bcl-2* transplanted lymphoma cells, or between the vehicle and W146-treated *Myc;Cre;bcl-2* lymphoma cells. *P* values that were equal to or less than 0.05 were considered statistically significant. *P*-values were not adjusted for multiple comparisons.

Supplementary Material

Refer to Web version on PubMed Central for supplementary material.

Acknowledgments

We thank M. Calicchio, Drs. L. Cameron, E. Payne, E. Breen, J. Struthers, G. Wei for technical help, advice and reagents, J. Gilbert for editorial advice, and B. Baker and R. Gilbert and K.P. Kotredes for fish care and husbandry. This work was supported by grants from the National Institutes of Health (CA068484, A.T.L.; K99CA134743, H.F.; NRSA T32-HL086344, D.L.S.; 1K08CA133103, A.G.; 1K01DK074555, C.A.J.; CA077429, J.R.T.; K01AR05562190-01A1 and 3K01AR055619-03S1, D.M.L.), the Leukemia & Lymphoma Society (H.F.), Prevent Cancer Foundation Postdoctoral Fellowship (D.L.S.), the William Lawrence Foundation (A.G.), and a Seed Grant from the Harvard Stem Cell Institute (D.M.L.). L.I.Z. is a founder and stock-holder of Fate, Inc. and a scientific advisor for Stemgent. A.T.L. is on the board of iLAB and a scientific advisor for OncoMed, Inc. The content of this research is solely the responsibility of the authors and does not necessarily represent the official views of the NIH.

References

- Asker C, Wiman KG, Selivanova G. p53-induced apoptosis as a safeguard against cancer. *Biochem Biophys Res Commun.* 1999; 265:1–6. [PubMed: 10548481]
- Amaravadi RK, Yu D, Lum JJ, Bui T, Christophorou MA, Evan GI, Thomas-Tikhonenko A, Thompson CB. Autophagy inhibition enhances therapy-induced apoptosis in a Myc-induced model of lymphoma. *J Clin Invest.* 2007; 117:326–336. [PubMed: 17235397]
- Bernard G, Zoccola D, Deckert M, Breittmayer JP, Aussel C, Bernard A. The E2 molecule (CD99) specifically triggers homotypic aggregation of CD4+ CD8+ thymocytes. *J Immunol.* 1995; 154(1): 26–32. [PubMed: 7527813]
- Cairo MS, Raetz E, Lim MS, Davenport V, Perkins SL. Childhood and adolescent non-Hodgkin lymphoma: new insights in biology and critical challenges for the future. *Pediatric blood & cancer.* 2005; 45:753–769. [PubMed: 15929129]
- Cao Y, Klionsky DJ. Physiological functions of Atg6/Beclin 1: a unique autophagy-related protein. *Cell Res.* 2007; 17:839–849. [PubMed: 17893711]
- Crist WM, Shuster JJ, Falletta J, Pullen DJ, Berard CW, Vietti TJ, Alvarado CS, Roper MA, Prasthofer E, Grossi CE. Clinical features and outcome in childhood T-cell leukemia-lymphoma according to stage of thymocyte differentiation: a Pediatric Oncology Group Study. *Blood.* 1988; 72:1891–7. [PubMed: 3058229]
- Dang CV, O'Donnell KA, Juopperi T. The great MYC escape in tumorigenesis. *Cancer Cell.* 2005; 8:177–178. [PubMed: 16169462]
- Donati A, Ventrucci A, Cavallini G, Masini M, Vittorini S, Chantret I, Codogno P, Bergamini E. In vivo effect of an antilipolytic drug (3,5'-dimethylpyrazole) on autophagic proteolysis and autophagy-related gene expression in rat liver. *Biochem Biophys Res Commun.* 2008; 366:786–792. [PubMed: 18082617]
- Eischen CM, Weber JD, Roussel MF, Sherr CJ, Cleveland JL. Disruption of the ARF-Mdm2-p53 tumor suppressor pathway in Myc-induced lymphomagenesis. *Genes Dev.* 1999; 13:2658–2669. [PubMed: 10541552]
- Feng H, Langenau DM, Madge JA, Quinkertz A, Gutierrez A, Neuberger DS, Kanki JP, Look A Thomas. Heat-shock induction of T-cell lymphoma/leukaemia in conditional Cre/lox-regulated transgenic zebrafish. *Br J Haematol.* 2007; 138:169–175. [PubMed: 17593023]
- Ferrando AA, Neuberger DS, Staunton J, Loh ML, Huard C, Raimondi SC, Behm FG, Pui CH, Downing JR, Gilliland DG, et al. Gene expression signatures define novel oncogenic pathways in T cell acute lymphoblastic leukemia. *Cancer Cell.* 2002; 1:75–87. [PubMed: 12086890]
- Ferrando AA. The role of NOTCH1 signaling in T-ALL. *Hematology Am Soc Hematol Educ Program.* 2009:353–61. [PubMed: 20008221]
- Goldberg JM, Silverman LB, Levy DE, Dalton VK, Gelber RD, Lehmann L, Cohen HJ, Sallan SE, Asselin BL. Childhood T-cell acute lymphoblastic leukemia: the Dana-Farber Cancer Institute acute lymphoblastic leukemia consortium experience. *J Clin Oncol.* 2003; 21:3616–3622. [PubMed: 14512392]

- Hoffman B, Amanullah A, Shafarenko M, Liebermann DA. The proto-oncogene c-myc in hematopoietic development and leukemogenesis. *Oncogene*. 2002; 21:3414–3421. [PubMed: 12032779]
- Kabeya Y, Mizushima N, Ueno T, Yamamoto A, Kirisako T, Noda T, Kominami E, Ohsumi Y, Yoshimori T. LC3, a mammalian homologue of yeast Apg8p, is localized in autophagosome membranes after processing. *Embo J*. 2000; 19:5720–5728. [PubMed: 11060023]
- Kawamura-Kodama K, Tsutsui J, Suzuki ST, Kanzaki T, Ozawa M. N-cadherin expressed on malignant T cell lymphoma cells is functional, and promotes heterotypic adhesion between the lymphoma cells and mesenchymal cells expressing N-cadherin. *J Invest Dermatol*. 1999; 112(1): 62–6. [PubMed: 9886265]
- Langenau DM, Jette C, Berghmans S, Palomero T, Kanki JP, Kutok JL, Look AT. Suppression of apoptosis by bcl-2 overexpression in lymphoid cells of transgenic zebrafish. *Blood*. 2005; 105:3278–3285. [PubMed: 15618471]
- Langenau DM, Traver D, Ferrando AA, Kutok JL, Aster JC, Kanki JP, Lin S, Prochownik E, Trede NS, Zon LI, Look AT. Myc-induced T cell leukemia in transgenic zebrafish. *Science*. 2003; 299:887–890. [PubMed: 12574629]
- Lin CI, Chen CN, Lin PW, Lee H. Sphingosine 1-phosphate regulates inflammation-related genes in human endothelial cells through S1P1 and S1P3. *Biochem Biophys Res Commun*. 2007; 355(4): 895–901. [PubMed: 17331465]
- Lum JJ, DeBerardinis RJ, Thompson CB. Autophagy in metazoans: cell survival in the land of plenty. *Nature reviews*. 2005; 6:439–448.
- Makgoba MW, Sanders ME, Ginther Luce GE, Dustin ML, Springer TA, Clark EA, Mannoni P, Shaw S. ICAM-1 a ligand for LFA-1-dependent adhesion of B, T and myeloid cells. *Nature*. 1988; 331(6151):86–8. [PubMed: 3277059]
- Meyer N, Kim SS, Penn LZ. The Oscar-worthy role of Myc in apoptosis. *Semin Cancer Biol*. 2006; 16:275–287. [PubMed: 16945552]
- Mootha VK, Lindgren CM, Eriksson KF, Subramanian A, Sihag S, Lehar J, Puigserver P, Carlsson E, Ridderstrale M, Laurila E, Houstis N, Daly MJ, Patterson N, Mesirov JP, Golub TR, Tamayo P, Spiegelman B, Lander ES, Hirschhorn JN, Altshuler D, Groop LC. PGC-1alpha-responsive genes involved in oxidative phosphorylation are coordinately downregulated in human diabetes. *Nat Genet*. 2003; 34:267–273. [PubMed: 12808457]
- Nesbit CE, Tersak JM, Prochownik EV. MYC oncogenes and human neoplastic disease. *Oncogene*. 1999; 18:3004–3016. [PubMed: 10378696]
- Nilsson JA, Cleveland JL. Myc pathways provoking cell suicide and cancer. *Oncogene*. 2003; 22:9007–9021. [PubMed: 14663479]
- Palomero T, Lim WK, Odom DT, Sulis ML, Real PJ, Margolin A, Barnes KC, O'Neil J, Neuberg D, Weng AP, et al. NOTCH1 directly regulates c-MYC and activates a feed-forward-loop transcriptional network promoting leukemic cell growth. *Proc Natl Acad Sci U S A*. 2006; 103:18261–18266. [PubMed: 17114293]
- Park MJ, Taki T, Oda M, Watanabe T, Yumura-Yagi K, Kobayashi R, Suzuki N, Hara J, Horibe K, Hayashi Y. FBXW7 and NOTCH1 mutations in childhood T cell acute lymphoblastic leukaemia and T cell non-Hodgkin lymphoma. *Br J Haematol*. 2009; 145:198–205. [PubMed: 19245433]
- Pear WS, Aster JC. T cell acute lymphoblastic leukemia/lymphoma: a human cancer commonly associated with aberrant NOTCH1 signaling. *Curr Opin Hematol*. 2004; 11:426–33. [PubMed: 15548998]
- Pelengaris S, Khan M, Evan G. c-MYC: more than just a matter of life and death. *Nat Rev Cancer*. 2002; 2:764–776. [PubMed: 12360279]
- Petrie HT, Zúñiga-Pflücker JC. Zoned out: functional mapping of stromal signaling microenvironments in the thymus. *Annu Rev Immunol*. 2007; 25:649–79. [PubMed: 17291187]
- Raetz EA, Perkins SL, Bhojwani D, Smock K, Philip M, Carroll WL, Min DJ. Gene expression profiling reveals intrinsic differences between T-cell acute lymphoblastic leukemia and T-cell lymphoblastic lymphoma. *Pediatric blood & cancer*. 2006; 47:130–140. [PubMed: 16358311]
- Rosen H, Goetzl EJ. Sphingosine 1-phosphate and its receptors: an autocrine and paracrine network. *Nat Rev Immunol*. 2005a; 5(7):560–70. [PubMed: 15999095]

- Rosen H, Gonzalez-Cabrera PJ, Sanna MG, Brown S. Sphingosine 1-phosphate receptor signaling. *Annu Rev Biochem.* 2009b; 78:743–68. [PubMed: 19231986]
- Sanna MG, Wang SK, Gonzalez-Cabrera PJ, Don A, Marsolais D, Matheu MP, Wei SH, Parker I, Jo E, Cheng WC, Cahalan MD, Wong CH, Rosen H. Enhancement of capillary leakage and restoration of lymphocyte egress by a chiral S1P1 antagonist in vivo. *Nat Chem Biol.* 2006; 8:434–41. [PubMed: 16829954]
- Sen L, Borella L. Clinical importance of lymphoblasts with T markers in childhood acute leukemia. *The New England journal of medicine.* 1975; 292:828–832. [PubMed: 1078713]
- Sharma VM, Calvo JA, Draheim KM, Cunningham LA, Hermance N, Beverly L, Krishnamoorthy V, Bhasin M, Capobianco AJ, Kelliher MA. Notch1 contributes to mouse T-cell leukemia by directly inducing the expression of c-myc. *Mol Cell Biol.* 2006; 26:8022–8031. [PubMed: 16954387]
- Shimizu D, Taki T, Utsunomiya A, Nakagawa H, Nomura K, Matsumoto Y, Nishida K, Horiike S, Taniwaki M. Detection of NOTCH1 mutations in adult T-cell leukemia/lymphoma and peripheral T-cell lymphoma. *Int J Hematol.* 2007; 85:212–218. [PubMed: 17483057]
- Sotsios Y, Ward SG. Phosphoinositide 3-kinase: a key biochemical signal for cell migration in response to chemokines. *Immunological reviews.* 2000; 177:217–235. [PubMed: 11138779]
- Stachura DL, Reyes JR, Bartunek P, Paw BH, Zon LI, Traver D. Zebrafish kidney stromal cell lines support multilineage hematopoiesis. *Blood.* 2009; 114:279–289. [PubMed: 19433857]
- Strasser A, Harris AW, Bath ML, Cory S. Novel primitive lymphoid tumours induced in transgenic mice by cooperation between myc and bcl-2. *Nature.* 1990; 348:331–333. [PubMed: 2250704]
- Tanaka S, Saito K, Reed JC. Structure-function analysis of the Bcl-2 oncoprotein. Addition of a heterologous transmembrane domain to portions of the Bcl-2 beta protein restores function as a regulator of cell survival. *Journal of Biochemistry.* 1993; 268:10920.
- Vousden KH. Switching from life to death: the Miz-ing link between Myc and p53. *Cancer Cell.* 2002; 2:351–352. [PubMed: 12450789]
- Weng AP, Ferrando AA, Lee W, Morris JP, Silverman LB, Sanchez-Irizarry C, Blacklow SC, Look AT, Aster JC. Activating mutations of NOTCH1 in human T cell acute lymphoblastic leukemia. *Science.* 2004; 306:269–271. [PubMed: 15472075]
- Weng AP, Millholland JM, Yashiro-Ohtani Y, Arcangeli ML, Lau A, Wai C, Del Bianco C, Rodriguez CG, Sai H, Tobias J, et al. c-Myc is an important direct target of Notch1 in T-cell acute lymphoblastic leukemia/lymphoma. *Genes Dev.* 2006; 20:2096–2109. [PubMed: 16847353]
- Westerfield. *The Zebrafish Book: A Guide for the Laboratory Use of Zebrafish (Brachydanio rerio).* 2.1. Eugene, OR: University of Oregon Press; 1994.
- Yan FP, Chen YJ, Huang XH. Expression of beclin1 and LC3 after rat's skin contusion. *Fa Yi Xue Za Zhi.* 2007; 23:11–13. [PubMed: 17330750]
- Yasmeen A, Berdel WE, Serve H, Muller-Tidow C. E- and A-type cyclins as markers for cancer diagnosis and prognosis. *Expert Rev Mol Diagn.* 2003; 3:617–633. [PubMed: 14510182]

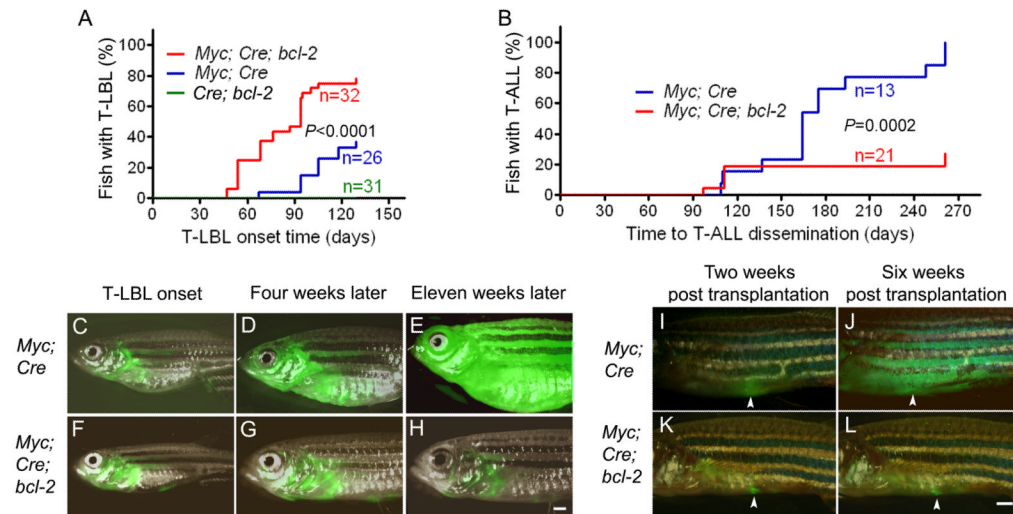


Figure 1. *Bcl-2* Promotes Onset but Inhibits the Progression of Myc-induced T-LBL in Zebrafish

(A) Rate of tumor onset in three transgenic zebrafish lines: *hsp70-Cre;rag2-EGFP-bcl-2* (*Cre;bcl-2*) double-transgenic fish (n=31; green line), *rag2-LDL-EGFP-Myc;hsp70-Cre* (*Myc;Cre*) double-transgenic fish (n=26; blue line), and *rag2-LDL-EGFP-Myc;hsp70-Cre;rag2-EGFP-bcl-2* (*Myc;Cre;bcl-2*) triple-transgenic fish (n=32; red line). (B) Rate of T-LBL progression to T-ALL in *Myc;Cre* (n=13; blue line) versus *Myc;Cre;bcl-2* (n=21; red line) transgenic fish. (C-H) Localized GFP-labeled tumors first arose as T-LBL in *Myc;Cre* (C; 112-day) and *Myc;Cre;bcl-2* (F; 119-day) transgenic fish; widespread dissemination leading to leukemia was seen within 11 weeks after T-LBL onset in *Myc;Cre* fish (D,E), but not in *Myc;Cre;bcl-2* triple transgenics (G,H). (I-L) GFP-positive T-LBL tumor cells (n=5 per group) transplanted into the peritoneum of irradiated wild-type hosts. Tumor cells from the *Myc;Cre* double-transgenic fish disseminated rapidly (I-J), while those from the *Myc;Cre;bcl-2* triple-transgenics remained localized (K-L). Scale bar for panels C-H and I-L = 1 mm. See also Figure S1.

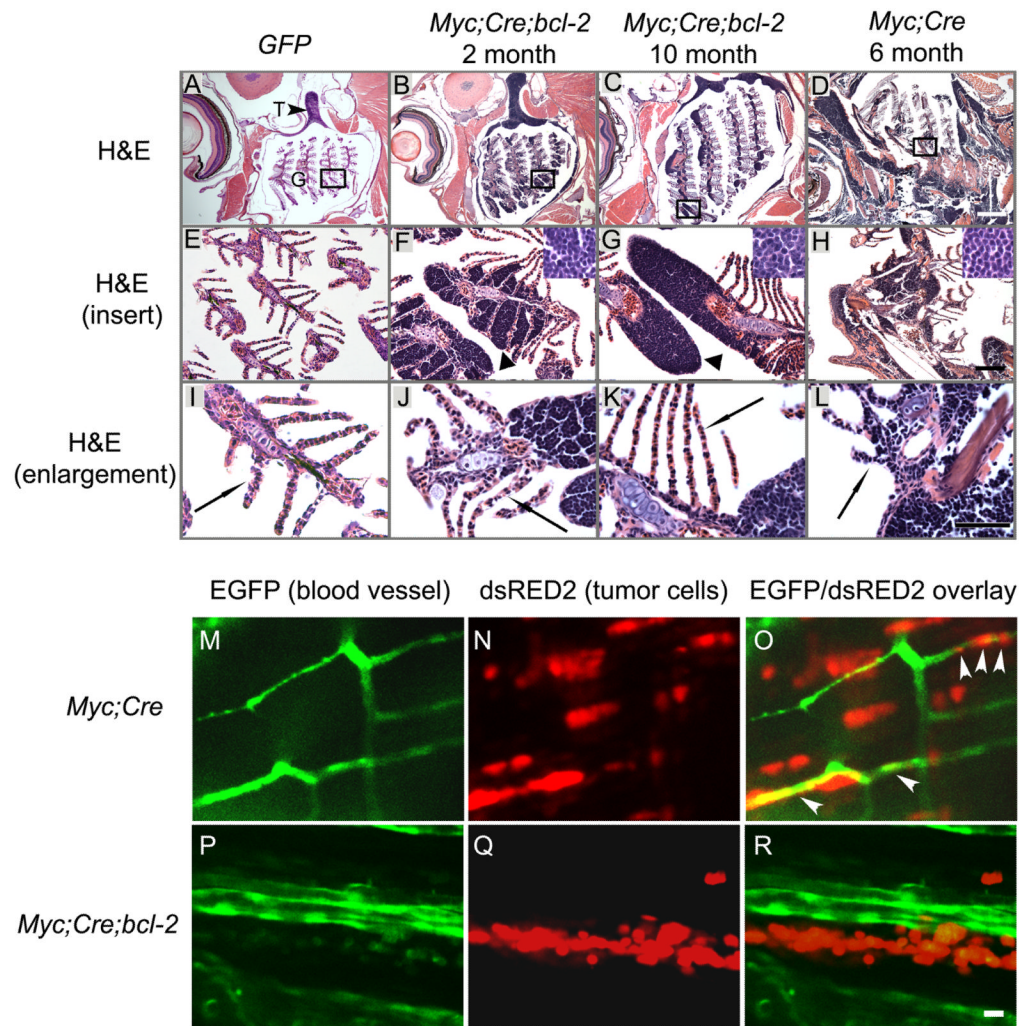


Figure 2. Zebrafish T-Lymphoblasts Overexpressing *Bcl-2* Spread Locally but Fail to Intravasate into Vasculature

(A,E,I) T cells in a control fish are restricted to the thymus above the gill arches and underneath the operculum (n=3). (B,C,F,G,J,K) GFP and dsRED2-positive tumor cells (arrowheads; F,G) in the *Myc;Cre;bcl-2* fish invade tissues outside the thymus and infiltrate local structures, including the primary lamellae (filaments) and cartilaginous gill rays by 2 months (B,F,J; n=3) but fail to invade vasculature by 10 months (C,G,K; n=3). By contrast, GFP- and dsRED2-expressing cells of the *Myc;Cre* transgenic fish (D,H,L; n=3) enter secondary lamellae that contain the capillary network (compare panels J-K with panel L, arrows) and disseminate widely throughout the host, infiltrating distant muscle and fat tissues by 6 months. Black arrowhead in panel A points to thymus (T) and the gill region is indicated (G). Inserts in panels F, G, and H show enlargements of tumor cells. (M,N,O) dsRED2-expressing lymphoma cells (N) from the *Myc;Cre* fish intravasate into EGFP-labeled vasculature (M) of the transplant host (*fli1-EGFP;Casper*) by 6 day post-transplantation (see arrowheads in O); (P,Q,R) In contrast, dsRED2-expressing lymphoma cells (Q) from the *Myc;Cre;bcl-2* fish fail to intravasate vasculature (P) of the transplant hosts by 6 day post-transplantation (compare panel R with O). Note aggregates of the *Myc;Cre;bcl-2* lymphoma cells in panels Q and R. Scale bar for panels A-D = 200 μ m; for panels E-H = 50 μ m; for panels I-L and M-R = 10 μ m. See also Figure S2.

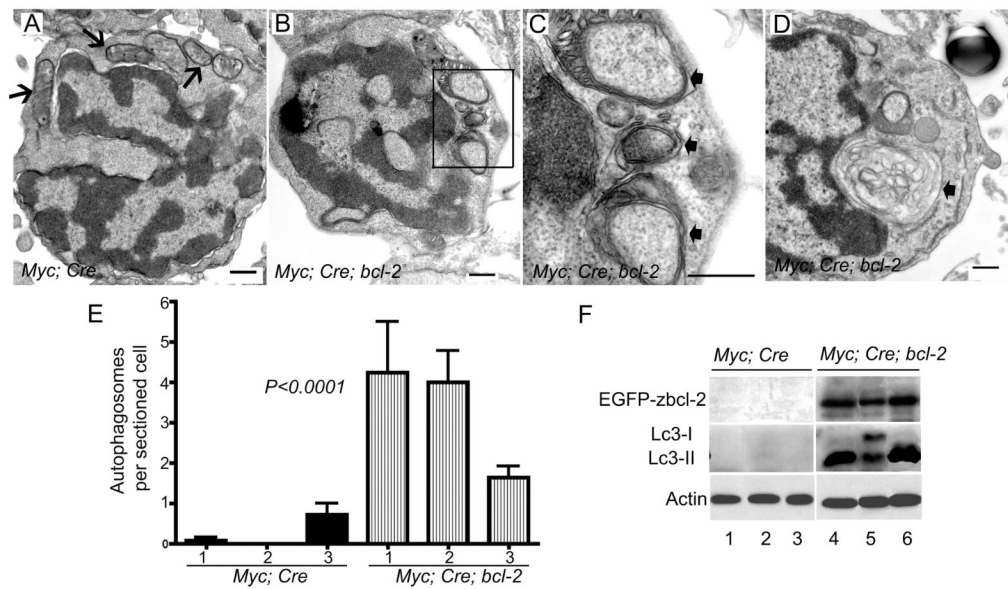


Figure 3. Zebrafish Lymphoblasts Overexpressing *Myc* and *Bcl-2* Undergo Autophagy (A) Electron microscopic analysis rarely identified autophagosomes in tumor cells from *Myc;Cre* transgenic fish. Mitochondria are indicated by arrows. (B-D) Thymic lymphoblasts from *Myc;Cre;bcl-2* triple-transgenics show prominent autophagosomes/ autolysophagosomes. Panel C is a magnified view of B (box). Arrows indicate double-membrane autophagosomes containing cytoplasm and cytoplasmic organelles. An autolysophagosome is shown in panel D (arrow). (E) Quantification of autophagosomes and autolysophagosomes in *Myc;Cre* (solid bars) and *Myc;Cre;bcl-2* (hatched bars) tumor cells were harvested from three individual fish. From 9 to 15 different cells from each fish were sectioned and analyzed. mean \pm SD results from three individual fish are shown. (F) Western blot analyses of the protein levels of EGFP-zbcl-2, Lc3-I, and Lc3-II in three individual *Myc;Cre* and *Myc;Cre;bcl-2* transgenic fish. Actin was used as a loading control in each lane. Scale bars for panels A-D = 500 nm. See also Figure S3.

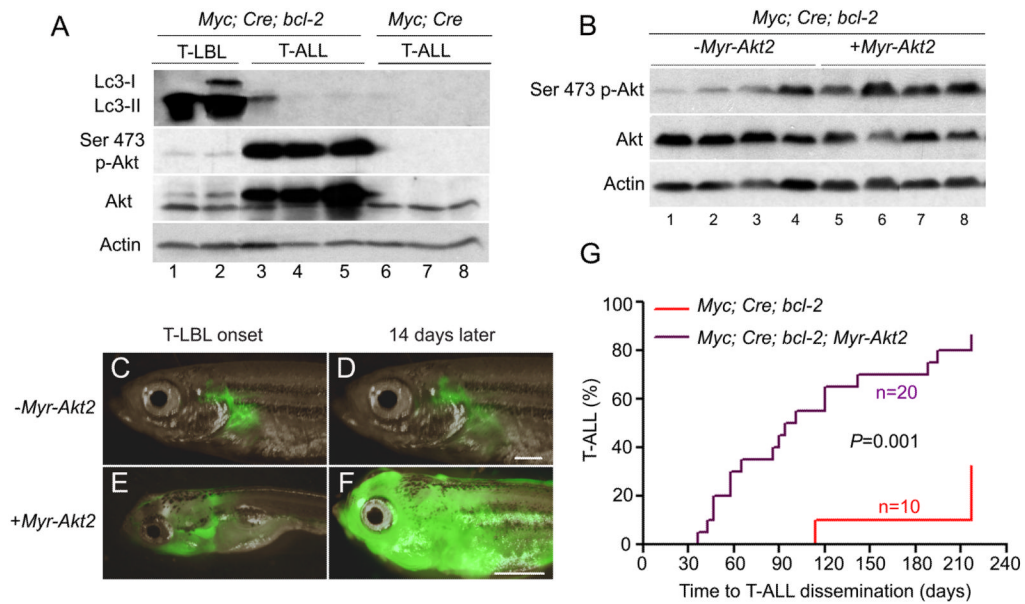


Figure 4. Akt Activation Promotes the Progression of T-LBL to T-ALL in *Myc;Cre;bcl-2* Transgenic Fish

(A) Western blot analysis of Lc3-I, Lc3-II, Ser473p-Akt, and Akt protein expression in zebrafish *Myc;Cre;bcl-2* lymphoma (two tumor samples) and leukemia (three tumor samples) cells and in zebrafish *Myc;Cre* leukemia cells (three tumor samples). (B) Western blot analysis of Ser473p-Akt and Akt expression in *Myc;Cre;bcl-2* (n=4) and *Myc;Cre;bcl-2;Myr-Akt2* (n=4) zebrafish lymphomas. (C-F) Upon constitutive activation of *Myr-Akt2*, *Myc;Cre;bcl-2* transgenic fish rapidly progress from T-LBL (E; T-LBL onset at 20 days) to T-ALL (F; at 34 days), compared with the *Myc;Cre;bcl-2* transgenic fish lacking *Myr-Akt2* expression (C-D). (G) Rate of T-LBL progression to T-ALL in *Myc;Cre;bcl-2* transgenic fish (n=10; red) and *Myc;Cre;bcl-2;Akt2* transgenic fish (n=20; purple). Actin protein levels in panels A-B served as loading controls. Scale bars for panels C-F = 1 mm. See also Figure S4.

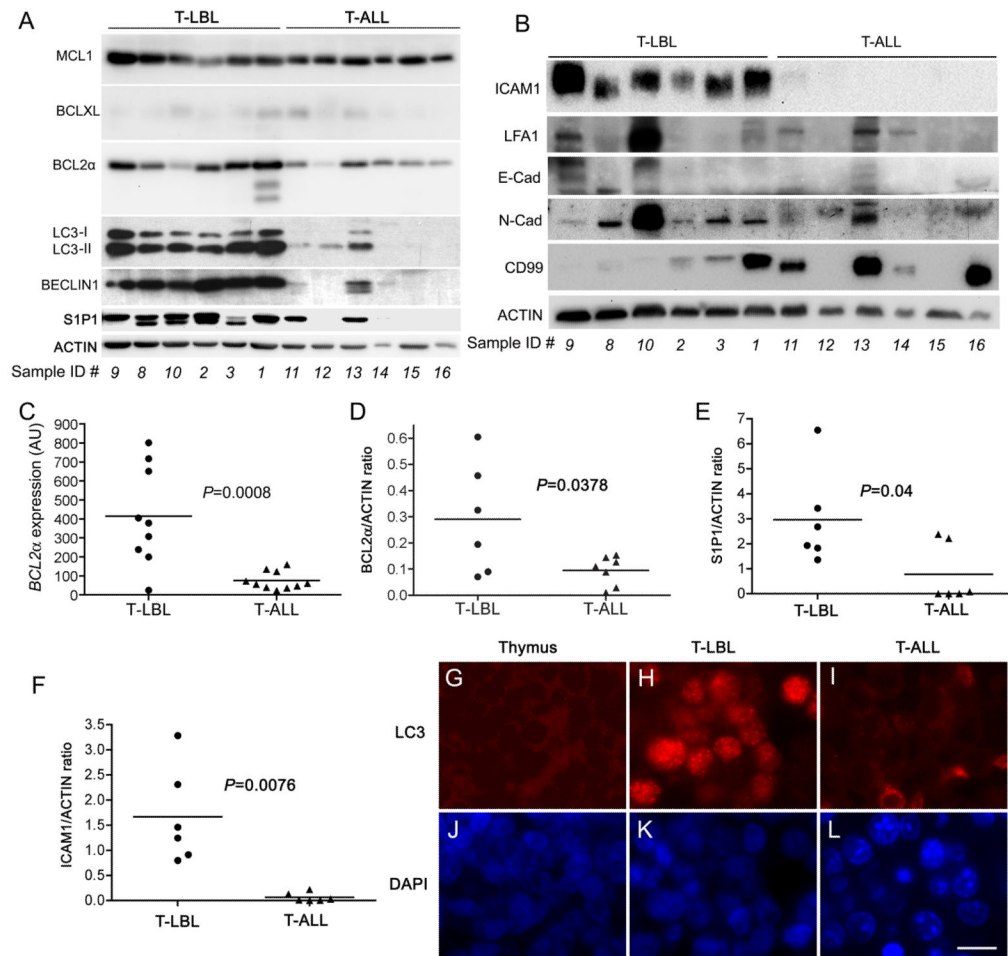


Figure 5. Human T-LBLs Undergo Autophagy and Overexpress *BCL2α*, *S1P1* and *ICAM1*
 (A) Western blot showing protein levels of MCL1, BCLXL, BCL2α, LC3-I, LC3-II, BECLIN 1, S1P1, and ACTIN in six T-LBL versus six T-ALL human patient samples. (B) Western blot showing the levels of ICAM1, LFA1, E-Cad, N-Cad, CD99, and ACTIN in 6 T-LBL versus 6 T-ALL human patient samples. (C) Gene expression profiling of human T-LBL and T-ALL samples shows that *BCL2α* is expressed at high levels in T-LBL but not T-ALL samples. (D) *BCL2α* versus ACTIN protein ratios demonstrating that *BCL2α* levels are significantly higher in human T-LBL samples compared with T-ALL samples (n=6 for T-LBL and n=7 for T-ALL; to view the Western blot, see Figure S5B). (E) *S1P1* versus ACTIN protein ratios demonstrating that *S1P1* protein levels are significantly higher in human T-LBL samples compared to T-ALL samples. (F) *ICAM1* versus ACTIN protein ratios demonstrating the significantly higher *ICAM1* in human T-LBL samples compared to T-ALL samples. (G-L) Immunofluorescent staining indicates the subcellular localization of LC3 in normal thymus (G), T-LBL (H), and T-ALL (I) cells. (J-L) DAPI staining of the cells shown in G-I, respectively. AU stands for arbitrary units. Bars denote median values. Scale bars for panels G-L = 10 μm. See also Figure S5 and Table S1.

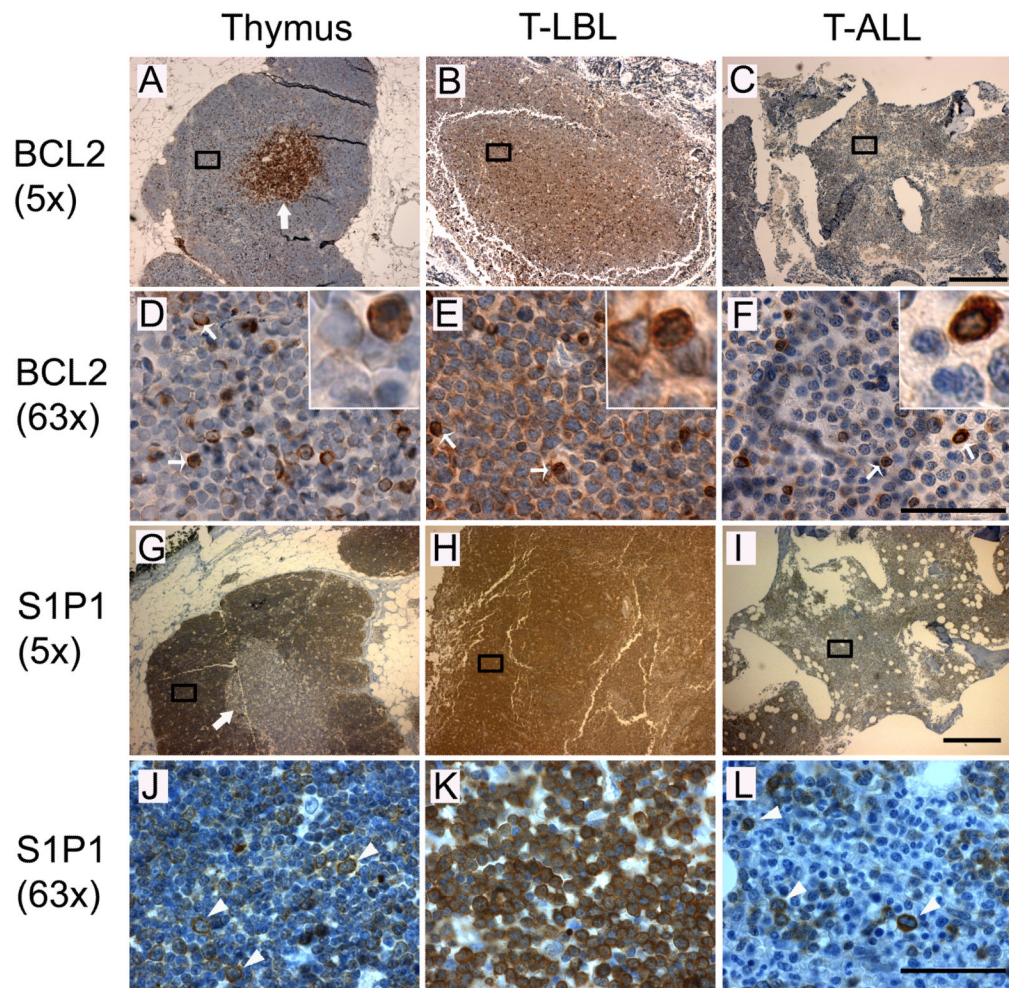
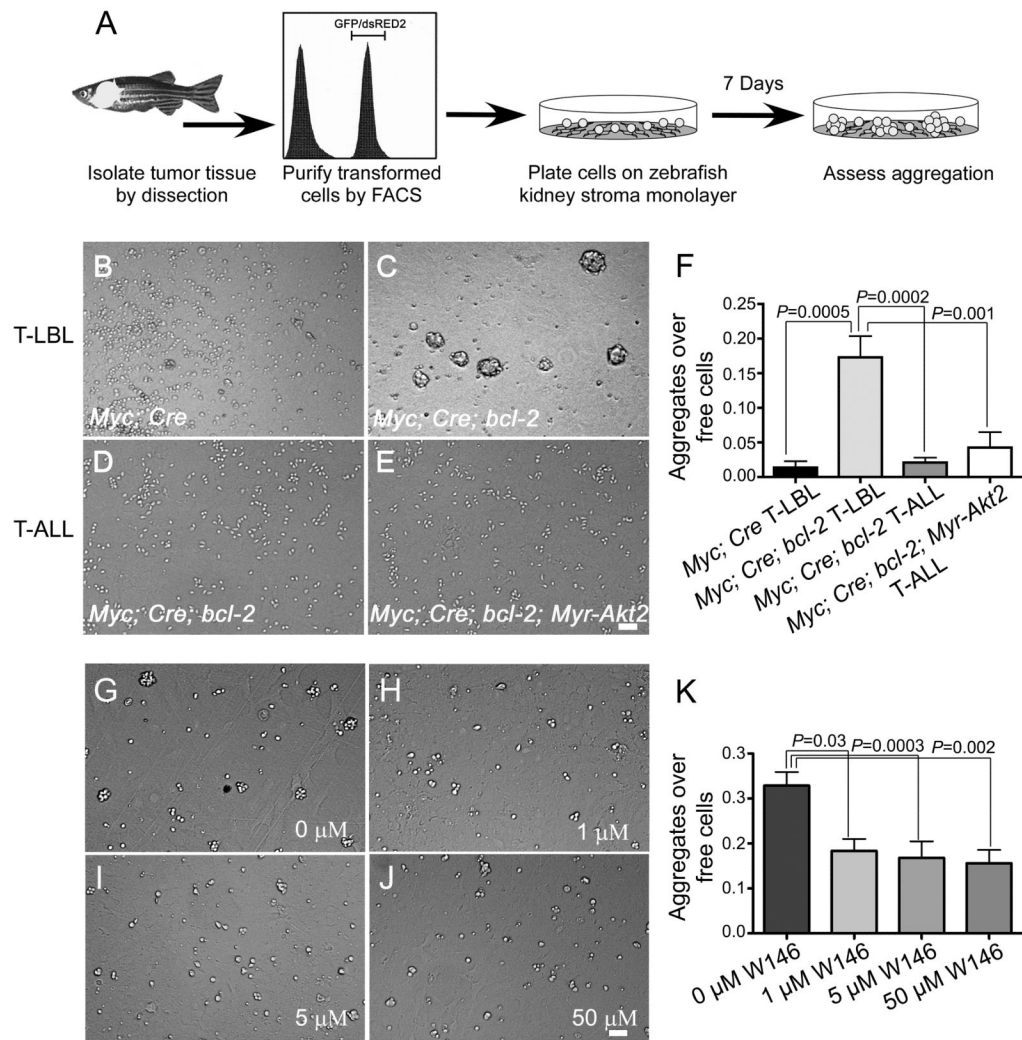


Figure 6. Immunohistochemical analysis of BCL2 and S1P1 in human T-LBL and T-ALL (A-F) Human BCL2 detected by immunohistochemistry in normal thymus (A,D) and in samples from patients with T-LBL (B,E) or T-ALL (C,F). Panels D-F are magnified views of boxes in A-C, respectively, and insets show individual cells including a mature thymocyte with high *BCL2* expression. (G-L) Human S1P1 detected by immunohistochemistry in normal thymus (G,J) and in samples from patients with T-LBL (H,K) and T-ALL (I,L). Panels J-L are magnified views of boxes in G-I, respectively. Note the reciprocal expression pattern of BCL2 and S1P1 in the thymic cortex and medulla regions. The thick arrow in panel (A,G) shows the thymic medulla region, while thin arrows in panels (D-F) indicate mature thymocytes with high *BCL2* expression, Arrowheads in panels (J-L) show the *S1P1* expression on the cortical thymocytes or lymphoblasts. Scale bars for panels A-C and G-I = 0.5mm; D-F and J-L = 50 μ m. See also Figure S6 and Table S2.



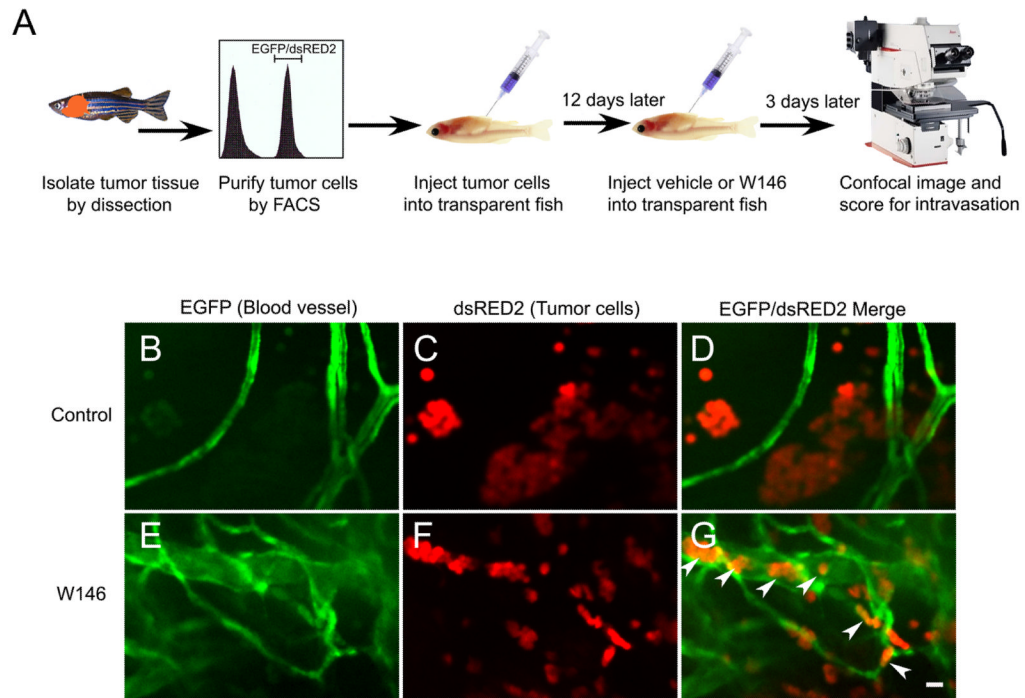


Figure 8. The Selective S1P1 Antagonist W146 Promotes Intravasation of *Bcl-2*-overexpressing T-LBL cells *in vivo*

(A) Schematic drawing of the experimental strategy. (B-G) Confocal images of EGFP-labeled blood vessels (B, E), dsRED2-labeled lymphoma cells (C,F), and the merged images of a vehicle-treated (D; n=29) and a W146-treated transplanted animal (G; n=18) demonstrate that W146 treatment promotes intravasation of *bcl-2*-overexpressing lymphoma cells (arrowheads) *in vivo* (compare panel G to D). Note that W146 treatment also inhibited the *in vivo* formation of lymphoma cell aggregates (compare panel F to C). Scale bar for panels B-G = 10 μ M.